Journal of Deep Learning, Computer Vision and Digital Image Processing
E-ISSN: 2986-8939 P-ISSN: 2986-8920
Vol. 4, No. 2, June 2026
DOI. https://doi.org/10.61255/decoding.v4i2.1525

Performance Evaluation and Comparative Analysis of Small Solar Panels for IoT Battery Charging Using ESP32 Microcontroller Platform

(Saddam Husein Siregar
Pusat Penelitian Kelapa Sawit, Medan, Indonesia)

(IzuKhairi Misrawi Rohali
Universitas Sumatera Utara, Medan, Indonesia)

(Mohamad Rifa Algifari Mulia Sembiring
Universitas Sumatera Utara, Medan, Indonesia)

(Sumaryanto
Pusat Penelitian Kelapa Sawit, Medan, Indonesia)

(Ratu Mutiara Siregar✉
Institut Teknologi Sawit Indonesia, Medan, Indonesia)

OPEN ACCESS

ARTICLE HISTORY
Received: May 3, 2026
Revised: June 18, 2026
Accepted: June 30, 2026

KEYWORDS
18650 battery;
ESP32;
Internet of Things;
Solar panel;
TP4056

ABSTRACT

Purpose – Small photovoltaic panels are widely used to support low-cost Internet of Things (IoT) sensor nodes; however, many locally available panels provide only nominal voltage labels without complete electrical specifications. This study evaluates the charging performance of three small solar panel configurations for a single 18650 lithium-ion battery used in an IoT-based monitoring node.
Methods – The experimental system used Lolin D32 boards based on ESP32, TP4056 charging modules, and identical battery connections. Node 1 used a large 9 V solar panel connected to a DC-DC step-down module calibrated to 5 V before entering the TP4056 input. Node 2 used a medium 6 V panel, while Node 3 used a mini solar panel directly connected to the charging module. Battery voltage was recorded every five minutes, converted into apparent state of charge (SoC), and uploaded to Google Sheets. The main field test was conducted from 10:00 to 15:00 on 8 June 2026.
Findings – Node 1 produced the highest apparent charging performance, with a charging rate of 12.8 percentage points per hour and a total SoC increase of 63.8 percentage points. In contrast, Node 2 and Node 3 each achieved only 0.5 percentage points per hour during the same test period.
Research implications – The findings indicate that nominal voltage alone is insufficient for selecting solar panels for IoT battery charging. Panel area, current capability, charger compatibility, firmware measurement sequence, and direct field validation must be considered.
Originality – This study provides practical field-based evidence for selecting small photovoltaic panels in low-cost IoT battery charging applications.

Correspondence Author: ✉ratu_ms@itsi.ac.id
To cite this article : Siregar, S. H., Rohali, I. K. M., Sembiring, M. R. A. M., Sumaryanto, & Siregar, R. M. (2026). Performance evaluation and comparative analysis of small solar panels for IoT battery charging using ESP32 microcontroller platform. Journal of Deep Learning, Computer Vision and Digital Image Processing, 4(2), 250–263. https://doi.org/10.61255/decoding.v4i2.1525

INTRODUCTION

Solar-powered Internet of Things (IoT) nodes are increasingly used for environmental monitoring, agricultural sensing, remote asset supervision, and field data acquisition because they can operate in locations where grid electricity is unreliable or unavailable. In these systems, the energy subsystem determines whether the sensing and communication functions can be sustained over time. A typical node depends on the interaction between the photovoltaic panel, storage battery, battery charger, voltage regulation stage, communication interval, sleep strategy, and measurement firmware. Previous studies have demonstrated that low-cost IoT architectures can monitor photovoltaic generation, climatic variables, battery behavior, and environmental conditions in real time [1]-[6]. Related work on wireless sensor networks has also shown that solar-powered sensor nodes can reduce battery replacement and support longer field deployment in soil water monitoring and distributed sensing applications [7], [8].

Despite this progress, component selection remains a practical challenge in small and low-cost IoT systems. Many small photovoltaic panels available in local electronic markets are sold with limited technical information. The label often provides only nominal voltage, whereas rated power, short-circuit current, maximum power current, active cell area, current-voltage characteristics, temperature coefficients, and recommended load conditions are not reported. For users who design inexpensive field nodes, this creates an important uncertainty: two panels with similar nominal voltage may produce substantially different charging responses once connected to a real battery charger and deployed under outdoor conditions. Therefore, relying only on a voltage label can lead to inappropriate panel selection, slow battery recovery, unstable node operation, or premature failure of the charging circuit.

The issue is also scientifically relevant because photovoltaic output is governed by more than open-circuit or nominal voltage. PV output changes with irradiance, module temperature, spectral condition, partial shading, panel orientation, internal resistance, and electrical operating point [9]-[15]. A small panel may show an acceptable open-circuit voltage when measured without load, but the voltage may collapse when the charger and the IoT node draw current. Conversely, a larger panel with higher nominal voltage may offer better current capability, yet it can exceed the safe input range of a lithium-ion charging module if no voltage regulation is used. This means that the usable charging performance is determined by system-level matching among the panel, regulator, charger, and battery rather than by a single label printed on the panel.

The ESP32 platform is attractive for low-cost solar-powered nodes because it integrates Wi-Fi connectivity, processing capability, analog-to-digital converter (ADC) channels, and low-power modes in a compact development board [16]-[19]. However, ESP32-based battery monitoring also has measurement limitations. Voltage-based state-of-charge estimation is sensitive to ADC calibration, battery relaxation behavior, load transients, and the nonlinear discharge curve of lithium-ion cells [16]-[21]. For this reason, apparent SoC derived from voltage should be interpreted as a comparative indicator unless it is supported by coulomb counting or calibrated battery models. In field experiments, the firmware sequence is also important because Wi-Fi transmission can create a transient voltage drop if battery voltage is read during communication rather than before radio activation.

Several studies have examined IoT-based photovoltaic monitoring, low-power data logging, battery monitoring, and online performance dashboards [22]-[26]. Rouibah et al. [4], for example, developed an IoT-based prototype for monitoring maximum PV output using measured electrical and environmental variables. Other studies have emphasized low-cost monitoring, real-time communication, data acquisition reliability, and measurement calibration [1]-[6], [22]-[24]. However, fewer studies focus on the preliminary selection of very small panels that lack complete manufacturer datasheets, especially by comparing multiple panel configurations using identical ESP32-based battery-charging nodes under the same field observation window. This gap is important for students, field technicians, and early-stage system developers who must choose components before they have access to laboratory-grade PV characterization equipment.

This study addresses that gap by comparing three small solar panel configurations for charging a single 18650 lithium-ion battery in an IoT monitoring node. The experimental system used identical Lolin D32 ESP32 boards, TP4056 lithium-ion charger modules, battery connections, and firmware sampling intervals. The independent variable was the solar panel configuration: a larger 9 V panel regulated through a step-down module, a medium 6 V panel connected directly to the charger input, and a mini panel connected directly to the charger input. Battery voltage was measured every five minutes, converted into apparent SoC, and uploaded to Google Sheets to support field monitoring and later comparison.

The theoretical contribution of this study is the clarification of solar-panel selection as a system-matching problem in low-cost IoT battery charging. Instead of treating nominal voltage as the main selection criterion, the study frames charging performance as the result of the interaction among active panel area, current capability under load, charger input requirements, voltage regulation, firmware measurement timing, and battery voltage response. The practical contribution is a field-oriented evaluation procedure that can help designers screen locally available small panels before deploying IoT nodes in agricultural, environmental, or remote monitoring applications. The findings are expected to support more reliable component selection, safer charger interfacing, and better data integrity in low-cost solar-powered IoT systems.

METHOD

Research design

This study used a comparative experimental design. Three IoT monitoring nodes were assembled with the same controller type, charger type, battery type, and sampling interval. The independent variable was the panel configuration. The observed response was the apparent battery SoC increase calculated from measured battery voltage. The field test used a fixed observation window from 10:00 to 15:00. Complete data for the three nodes were available on 8 June 2026. Additional supporting data for Node 2 and Node 3 were available on 7 June 2026. The 8 June data became the main comparison because all nodes were recorded in the same time window. The 7 June data were used only to show daily variation.

Irradiance, ambient temperature, panel temperature, charging current, and matched initial battery conditions were not controlled with laboratory instruments. Accordingly, the test should be interpreted as a practical field-screening comparison under shared outdoor conditions, not as a controlled PV efficiency or true energy-transfer experiment.

Hardware configuration

Each node consisted of a solar panel, a TP4056 lithium-ion charging module, one 18650 battery in a holder, and a Lolin D32 board based on ESP32. The battery holder output was connected to the TP4056 battery terminals for charging and to the Lolin D32 battery input for powering the controller. This connection allowed the ESP32 to remain active from the battery when solar input was unavailable.

Figure 1. Field placement of the three small solar panels during comparative testing.

Table 1. Configuration of the tested IoT monitoring nodes

Component	Node 1	Node 2	Node 3
Solar panel	9 V large panel	6 V medium panel	Mini panel
Approximate size	150 x 100 mm	120 x 80 mm	110 x 110 mm
Step-down module	Used, calibrated to 5 V	Not used	Not used
TP4056 input	From step-down output	Directly from panel	Directly from panel
Battery	18650 lithium-ion cell	18650 lithium-ion cell	18650 lithium-ion cell
Controller	Lolin D32 ESP32	Lolin D32 ESP32	Lolin D32 ESP32

Source: Primary field experiment, 2026.

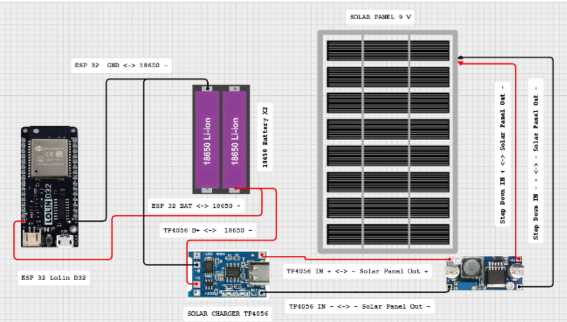

(a) Node 1 (9 V large panel with step-down)

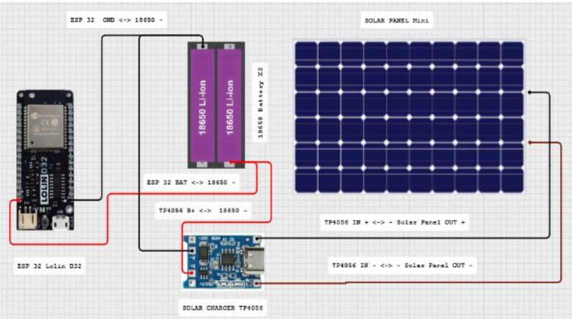

(b) Node 2 (6 V medium panel without step-down)

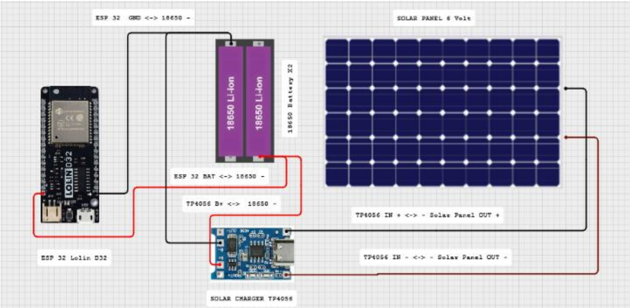

(c) Node 3 (mini panel without step-down)

Figure 2. Electrical configurations of the three IoT monitoring nodes: (a) Node 1 with a 9 V large solar panel connected through a DC-DC step-down converter to the TP4056 charger, (b) Node 2 with a 6 V medium panel directly connected to the TP4056 charger, and (c) Node 3 with a mini panel directly connected to the TP4056 charger.

Data acquisition and calibration

The sampling cycle began when the Lolin D32 woke from deep sleep. The firmware read battery voltage before Wi-Fi activation. This sequence was selected to reduce transient voltage-drop bias because Wi-Fi transmission increases instantaneous current demand. After the ADC reading, the board activated Wi-Fi, uploaded data to Google Sheets, and returned to deep sleep for five minutes.

Battery voltage was converted into apparent SoC using a simple linear mapping. The lower boundary was 3.2 V, and the upper boundary was 4.2 V. The formula was used only for comparison between panel configurations and was not treated as a coulomb-counted capacity measurement. The apparent SoC was calculated using (1).

$$SoC\ (\%) = ((V_{bat} - 3.2) / (4.2 - 3.2)) \times 100 \quad (1)$$

Values outside the 0-100% range were clipped. Manual ADC calibration was performed by comparing the ESP32 raw ADC value with a multimeter reading at the battery terminal. The calibration factor applied in the test was 0.001733, with a reported reading difference below 0.02 V after calibration.

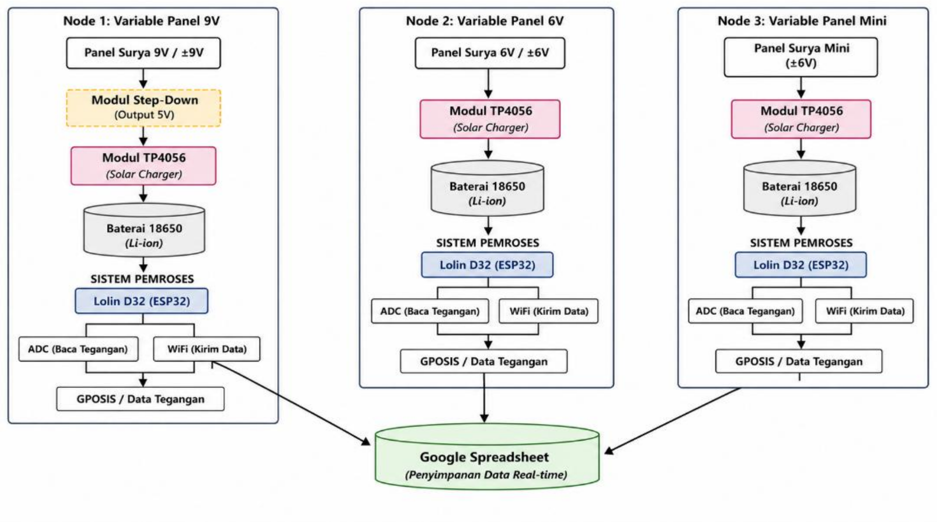

Figure 3. Overall data-flow architecture of the IoT monitoring system. Each monitoring node measured battery voltage, processed the data using the Lolin D32, and transmitted the records to Google Sheets for real-time monitoring.

Data analysis

The main performance metrics were average apparent charging rate and total apparent SoC increase. Average charging rate was obtained by dividing total SoC increase by the five-hour observation window. Total SoC increase was calculated from the difference between final and initial apparent SoC.

During early logging, anomalous records at 4.2 V appeared in the uncleaned log. They were traced to old SPIFFS-stored records uploaded after Wi-Fi reconnection and were generated before ADC calibration was finalized. Because the uncleaned SPIFFS buffer was overwritten after the firmware revision, the exact number of deleted 4.2 V records and their affected node/date could not be reconstructed from the archived cleaned dataset. The final analytical dataset therefore retained only current sampling records, and the firmware logic was revised to upload only the current sampling record.

RESULTS AND DISCUSSION

Apparent charging performance comparison

The three nodes showed different charging responses. On 8 June 2026, Node 1 increased from 5.3% to 69.1% apparent SoC during the 10:00–15:00 observation window. The total increase reached 63.8 percentage points, equivalent to an average charging rate of 12.8 percentage points per hour. In contrast, Node 2 increased by only 2.4 percentage points, while Node 3 increased by 2.5 percentage points within the same observation window.

Supporting observations collected on 7 June 2026 showed higher charging responses for Node 2 and Node 3 than those recorded on 8 June. Node 2 reached 1.8 percentage points per hour, while Node 3 reached 1.5 percentage points per hour. This difference indicates that daily irradiance, cloud cover, panel orientation, and battery condition may have influenced the charging response. Since the system did not record irradiance and charging current, these daily differences should be interpreted cautiously.

Table 2. Apparent battery charging performance during the test window

Node	panel	Nominal voltage	Panel size	Date	Rate (% point/hour)	Total increase (% point)
Node 1	large panel	9 V	150 x 100 mm	8 Jun	12.8	63.8

Node	panel	Nominal voltage	Panel size	Date	Rate (% point/hour)	Total increase (% point)
Node 2	medium panel	6 V	120 x 80 mm	8 Jun	0.5	2.4
Node 3	mini panel	Approx. 6 V	110 x 110 mm	8 Jun	0.5	2.5
Node 2	medium panel	6 V	120 x 80 mm	7 Jun	1.8	8.8
Node 3	mini panel	Approx. 6 V	110 x 110 mm	7 Jun	1.5	7.3

Source: Primary field experiment, 2026.

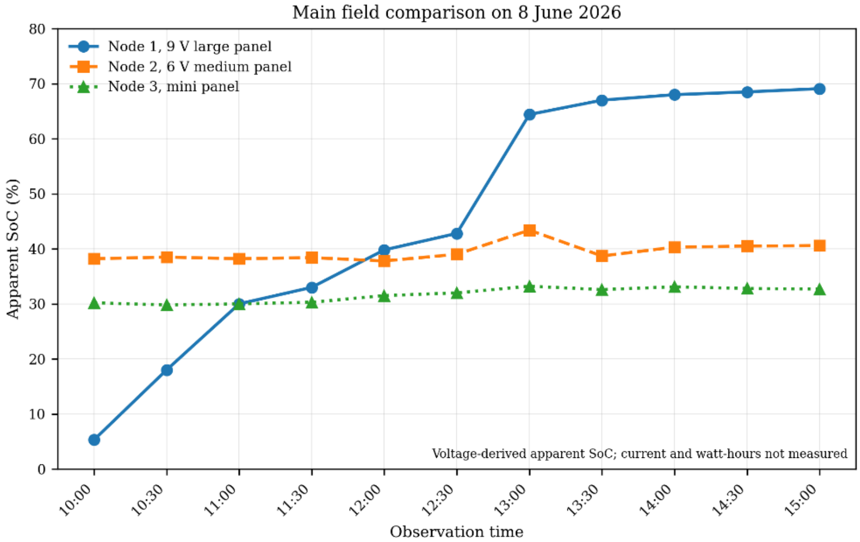

Figure 4. Apparent battery State of Charge (SoC) trends of the three tested solar-panel configurations during the cleaned main field-monitoring comparison on 8 June 2026 from 10:00 to 15:00. Values represent voltage-derived apparent SoC, not measured watt-hour storage.

Figure 4 presents the main comparison based on direct measurements collected from all three nodes within the same observation window after removal of obsolete buffered records. The figure shows that Node 1 had a substantially greater apparent SoC increase than Node 2 and Node 3 during the five-hour test period.

Supporting observations were also collected on 7 June 2026 for Node 2 and Node 3. On that day, Node 2 increased by 8.8 percentage points, corresponding to an apparent charging rate of 1.8 percentage points per hour, while Node 3 increased by 7.3 percentage points, corresponding to 1.5 percentage points per hour. These observations indicate that the charging response of the smaller panels varied across days. However, the 7 June results were treated as supporting data because complete direct measurements for all three nodes were not available within the same observation window.

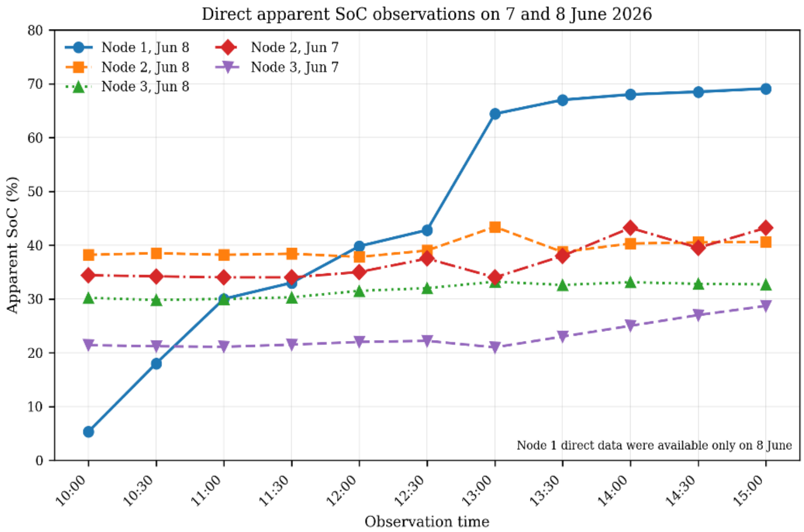

Figure 5. Direct apparent State of Charge (SoC) trends recorded during field monitoring on 7 and 8 June 2026. Direct measurements were available for all three nodes on 8 June 2026. On 7 June 2026, direct measurements were available for Node 2 and Node 3 only; no estimated Node 1 curve is included in this figure.

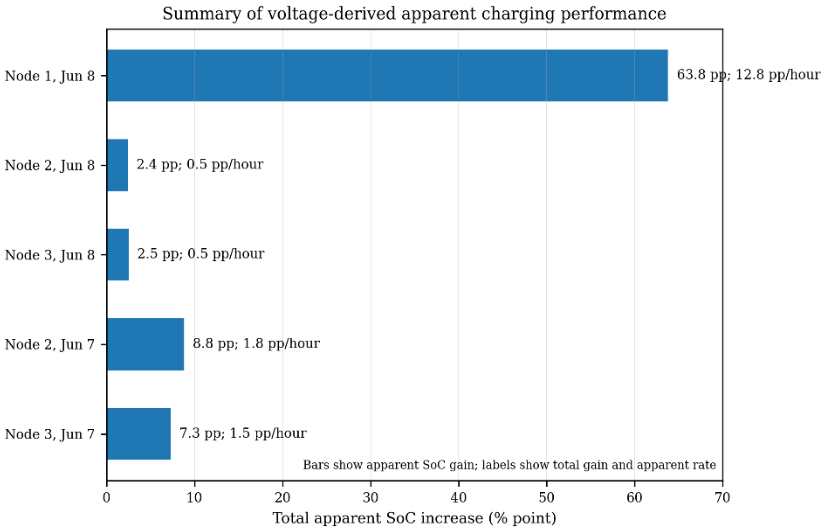

Figure 6. Summary of apparent charging rate and total apparent SoC increase for the tested solar-panel configurations, calculated from voltage-derived apparent SoC. Because current and watt-hour transfer were not measured, the bars represent apparent charging performance.

Figure 6 summarizes the cleaned analytical results reported in Table 2 using a publication-style chart rather than a dashboard screenshot. The values for Node 2 and Node 3 on 7 June 2026 are shown as supporting daily observations, while the main same-window comparison remains the 8 June 2026 dataset. The chart should be interpreted cautiously because it reflects apparent charging performance derived from battery voltage rather than measured current or energy transfer.

Technical interpretation of apparent charging performance

The result suggests that nominal voltage is not sufficient to predict apparent charging performance under the tested field conditions. Node 1 performed much better in the voltage-derived comparison because the panel had larger active area and likely higher current capability. The 9 V label did not directly determine the apparent battery charging rate. Rather, the useful charging response depended on the panel output current under load and the way the panel was matched with the charging circuit. This finding is consistent with photovoltaic models that link panel output to irradiance, temperature, and electrical operating point [13]-[15].

Node 1 required a DC-DC step-down module because a 9 V panel can exceed the safe input range of a TP4056 charger module. The step-down converter was calibrated to 5 V before the TP4056 input. Node 2 and Node 3 could be connected directly to TP4056 because their panel voltages were lower. This difference has a practical implication. A higher-voltage small panel may charge faster, but it needs voltage regulation to protect the charger and stabilize the input path. The firmware sequence also affected measurement quality. Reading the ADC before Wi-Fi activation reduced the possibility of voltage drop during measurement. This design choice is relevant for ESP32-based nodes because wireless transmission increases instantaneous current consumption. The use of deep sleep, short active time, and periodic upload supports low-power operation, as recommended in prior low-power IoT and data logging studies [16]-[19], [22]-[24].

The study still has methodological limitations. It measured battery voltage and apparent SoC but did not measure charging current, watt-hour transfer, panel irradiance, ambient temperature, or panel temperature. It also did not equalize battery initial conditions using laboratory-grade capacity, aging, or internal-resistance matching. As a result, the analysis cannot calculate true energy transfer, conversion efficiency, or exact charger efficiency. Future testing should include current sensors such as INA219 or ACS712, a calibrated irradiance sensor, panel temperature monitoring, and matched battery preparation. These additions would allow energy-based comparison and stronger statistical validation [25]-[30].

Data integrity and system improvement

The anomalous 4.2 V records show that cloud-based IoT logging requires clear metadata and an auditable cleaning log. A buffered record should include timestamp, firmware version, calibration factor, node identifier, and upload status. Without these fields, delayed uploads can mix obsolete readings with valid records. The corrected firmware removed unverified SPIFFS buffering and used direct upload from the current sampling cycle.

The proposed system remains useful as a low-cost preliminary screening tool. It helps users compare small panels under real field conditions before selecting components for longer deployments. However, a journal-level follow-up should add repeated trials, weather logging, current measurement, and error analysis to improve reproducibility.

Comparison with previous studies

The observed pattern is consistent with previous photovoltaic monitoring studies, but it extends them in a more component-selection-oriented direction. Studies on IoT-based PV monitoring have generally emphasized the ability of low-cost sensing systems to acquire voltage, current, irradiance, temperature, and power data from photovoltaic installations [1]-[6]. Rouibah et al. [4] monitored maximum output power and implemented multiple MPPT algorithms in a low-cost IoT prototype, while Demir [3] developed a monitoring system for stand-alone PV plant performance and power estimation. These studies show that low-cost controllers can support meaningful PV diagnostics when the measured variables are sufficiently complete. The present study differs because it evaluates a simpler and more constrained case: small panels without complete datasheets, one-cell lithium-ion charging, TP4056 charger modules, and ESP32-based field logging. The comparison therefore shifts attention from monitoring a mature PV installation to choosing an appropriate small panel before a low-cost IoT node is deployed.

The results also align with energy-harvesting literature showing that the performance of wireless sensor nodes depends on the balance between harvested energy, stored energy, and load demand [9]-[12]. In energy-harvesting wireless sensor networks, the availability of energy is not constant; it depends on weather, season, node duty cycle, communication load, and conversion losses. The low charging rates of Node 2 and Node 3 on 8 June indicate that a panel can be electrically compatible with a charger input but still deliver insufficient recoverable energy during the observation window. This point is important because direct compatibility should not be confused with practical adequacy. A panel that can start a charger may still fail to restore the battery fast enough to sustain repeated Wi-Fi uploads, especially when solar conditions are variable.

The comparison with studies on solar-powered wireless sensors is also instructive. Tsiropoulos et al. [7] compared battery- and solar-powered sensors for soil water monitoring and highlighted the relevance of power source selection for field sensing reliability. Haroun et al. [8] examined self-powered wireless sensor transmission supported by indoor solar energy harvesting. Those works demonstrate that solar support can reduce maintenance burden, but they also imply that the harvesting source must be sized according to the actual energy demand. The present results provide a small-scale example of that principle. Node 1 produced a clear apparent SoC increase, whereas Node 2 and Node 3 produced only marginal increases in the common test window. Therefore, a solar-powered IoT node should not be described as self-sustaining merely because it has a panel; the panel must be able to generate usable charging current under realistic load and environmental conditions.

Scientific interpretation of Node 1 apparent performance

Node 1 likely performed better because it combined larger collection area, higher voltage headroom, and regulated charger input. The approximate panel size of Node 1 was 150 x 100 mm, larger than the 120 x 80 mm medium panel and different from the smaller mini-panel configuration. Although active cell area alone does not fully determine output power, it usually increases the amount of incident solar energy that can be converted under the same irradiance. A larger panel also tends to provide greater current capability if the cell quality and construction are comparable. This is consistent with PV models that explain output power as a function of irradiance, temperature, and electrical operating point [13]-[15]. In practical terms, the 9 V label was not the direct reason for the faster charging; the advantage was more likely the ability of the larger panel to maintain usable voltage and current when connected through the regulator and charger.

The step-down module in Node 1 is a key part of the interpretation. A TP4056 charger is normally intended for a 5 V input path, and a 9 V panel connected directly may expose the charger module to unsuitable voltage conditions [29]. By calibrating the step-down output to 5 V before the TP4056 input, Node 1 separated the higher panel-side voltage from the charger-side requirement. This arrangement created two benefits. First, it protected the charger input from excessive voltage. Second, it allowed the panel to operate with more headroom under changing sunlight, while the charger received a more stable voltage level. Node 2 and Node 3 did not require a step-down converter from a voltage-safety perspective, but their direct connection also meant that any drop in panel output under load was seen directly by the charger input.

A further explanation is related to load matching. Small PV panels can show acceptable open-circuit voltage, yet their voltage decreases sharply when current is drawn. If the panel cannot supply enough current to maintain the charger input, the TP4056 charging process becomes weak or intermittent. In that situation, the battery voltage may rise only slightly during the observation window, as seen in Node 2 and Node 3. Node 1 had a better chance of keeping the charger in a useful operating region because the panel had greater apparent energy availability and the step-down converter provided regulated input. The observed difference between 12.8 percentage points per hour and 0.5 percentage points per hour should therefore be interpreted as a system-level outcome rather than as a simple comparison of voltage labels.

Battery state also influences the apparent charging rate. Node 1 started from a lower apparent SoC than the other nodes, and lithium-ion charging behavior is generally faster in the constant-current region than near the upper-voltage region [16]-[18], [29]. This means that part of the high apparent increase may be associated with the initial battery condition. However, this factor does not fully remove the practical significance of the result. Even if initial SoC affected the slope, the magnitude of the difference between Node 1 and the other nodes was very large. The smaller panels showed limited recovery in the same time window, while Node 1 moved from a low apparent SoC to a usable range. A stronger follow-up design should equalize initial SoC, use matched battery cells, and record current to separate panel performance from battery-state effects.

Interpretation of apparent SoC and measurement reliability

The use of voltage-derived apparent SoC should be interpreted carefully. Voltage-to-SoC mapping is simple and useful for field comparison, but it does not provide the same accuracy as coulomb counting or model-based estimation. Reviews of lithium-ion SoC estimation emphasize that battery voltage is affected by hysteresis, internal resistance, temperature, relaxation time, aging, and load history [16]-[18]. In this study, the linear 3.2 V to 4.2 V mapping was suitable as a comparative screening metric because all nodes used the same conversion method. However, it should not be read as an exact capacity measurement. The phrase apparent SoC is therefore important: it signals that the value represents a voltage-based estimate for comparison among configurations rather than a calibrated measure of stored energy in watt-hours.

The firmware measurement sequence improved the reliability of this simple metric. Reading battery voltage before Wi-Fi activation reduced the risk that radio transmission would pull the battery voltage downward during ADC sampling. This is consistent with ESP32 design considerations because Wi-Fi communication increases instantaneous current consumption and the platform provides low-power operating modes that can be used to reduce average energy demand [19], [27], [28]. The use of deep sleep, short active intervals, and periodic uploads therefore supports the energy-management logic described in low-power IoT and data-logging studies [19], [22]-[24]. For future systems, the same principle can be extended by adding repeated ADC sampling, median filtering, timestamped calibration constants, and battery-rest detection before SoC conversion.

The anomalous 4.2 V records also provide an important methodological lesson. In IoT systems, data quality depends not only on sensors but also on buffering, reconnection logic, timestamps, and firmware version control. The old SPIFFS-stored records created a misleading appearance of full battery voltage because obsolete readings were uploaded after reconnection. Removing those records from the analytical dataset was necessary, but the more general lesson is that each cloud record should carry metadata that supports auditability. At minimum, a field-deployed node should upload measurement timestamp, upload timestamp, firmware version, calibration factor, node identifier, data-source status, and battery-reading method. Without this metadata, delayed uploads can be mistaken for current measurements, which weakens reproducibility and makes peer review more difficult.

Theoretical and practical implications

Theoretically, this study supports a system-integration view of low-cost solar IoT design. The main unit of analysis is not the panel alone, the charger alone, or the controller alone, but the interaction among them. This interpretation is consistent with broader energy-harvesting research, which treats energy availability as a function of harvesting source, conversion pathway, storage behavior, load profile, and control policy [9]-[12]. The findings show that nominal panel voltage is an incomplete design variable. A more appropriate theoretical model for small solar IoT nodes should include at least five linked variables: available solar input, panel output under load, voltage regulation behavior, charger compatibility, and node energy consumption. The Node 1 result illustrates how an apparently simple hardware change can shift the whole operating point of the charging subsystem.

Practically, the findings recommend a more disciplined selection process for small solar panels. Designers should first identify the expected daily energy demand of the IoT node, including wake-up time, sensor reading, Wi-Fi connection, data upload, and sleep current. They should then test candidate panels under load rather than relying only on open-circuit voltage. A useful field screening protocol should measure panel voltage, charger input voltage, battery voltage, and charging current at repeated intervals across several weather conditions. If a higher-voltage panel is used, the input path should include a suitable regulator before the TP4056 or any equivalent lithium-ion charger. The result from Node 1 suggests that a regulated larger panel can be a better option than a smaller direct-connected panel, but only when the regulator and charger are matched safely.

The study also has implications for low-cost agricultural and environmental monitoring. Field nodes are often deployed by users who need inexpensive hardware and may not have access to laboratory PV test equipment. For these users, the most valuable output is not a perfect PV efficiency curve but a practical answer to whether the chosen panel can restore the battery during the available sunlight period. The five-hour observation window used here provides that kind of preliminary evidence. However, the method should be treated as an early screening tool. Before long-term deployment, the selected configuration should be tested for several days, including cloudy periods, different panel orientations, and different communication intervals.

Limitations

Several limitations should be acknowledged. First, the study used apparent SoC derived from battery voltage and did not measure charging current or energy transfer in watt-hours. This limits the ability to calculate true charging efficiency, panel energy yield, or charger conversion losses. Second, irradiance, ambient temperature, panel temperature, panel angle, charging current, and matched battery initial conditions were not controlled with laboratory instruments. Complete data for all three nodes were available only on 8 June 2026, while 7 June data were available only for Node 2 and Node 3. Therefore, daily irradiance, cloud cover, temperature, panel angle, cell capacity, aging, internal resistance, and starting SoC may have affected the observed apparent SoC responses. Third, the panel datasheets were unavailable, so exact rated power, short-circuit current, maximum power point voltage, and maximum power point current could not be compared.

These limitations do not invalidate the main conclusion, but they define the boundary of the claim. The study can confidently state that, under the tested field conditions and with the implemented hardware, Node 1 produced the highest apparent charging performance. It cannot yet claim a universal performance ranking for all 9 V, 6 V, or mini solar panels. It also cannot quantify the exact contribution of panel area, regulator efficiency, irradiance, temperature, and battery state as separate causal factors. A skeptical reader would therefore be correct to ask for repeated trials, current measurements, and environmental measurements before treating the result as a general engineering rule. The value of the present work lies in identifying the practical risk of voltage-label-based panel selection and demonstrating a low-cost procedure for detecting that risk.

Directions for future studies

Future studies should move from voltage-response screening toward energy-based characterization. Adding an INA219 or similar bidirectional current and power monitor would allow simultaneous measurement of panel-side current, charger input current, battery-side charging current, and bus voltage [30]. A calibrated irradiance sensor and panel temperature sensor should also be added so that charging performance can be normalized against environmental conditions [13]-[15]. With these additions, researchers could calculate watt-hours delivered to the charger, watt-hours stored in the battery, conversion losses, and apparent system efficiency. Repeated trials over multiple days would also allow statistical comparison among panels and help distinguish weather variation from hardware performance.

A second direction is firmware and power-policy optimization. The ESP32 supports several power-management modes, and communication frequency strongly affects energy demand [19], [27], [28]. Future work should test different upload intervals, deep-sleep durations, Wi-Fi reconnection strategies, and local buffering methods. A useful follow-up would compare whether reducing the upload frequency allows Node 2 or Node 3 to sustain operation despite their lower apparent charging rates. This would shift the design question from which panel appears to charge fastest to which combination of panel size, battery capacity, and duty cycle can maintain energy-neutral operation under measured energy conditions.

A third direction is charger and regulator comparison. The TP4056 is attractive because it is inexpensive and widely available, but it is a linear lithium-ion charger and may not be optimal for all solar applications [29]. Future studies could compare TP4056 modules with solar-oriented charger ICs, buck converters, buck-boost converters, and maximum power point tracking approaches. Such work would connect the practical field-screening focus of this study with the richer PV monitoring and MPPT literature [3], [4], [14]. It would also provide clearer guidance for designers who must choose between simplicity, cost, safety, and charging efficiency.

CONCLUSION

This study compared three small solar panel configurations for charging an 18650 lithium-ion battery in an ESP32-based IoT monitoring node. The large 9 V panel regulated through a 5 V step-down module produced the highest apparent charging performance, reaching 12.8 percentage points per hour and 63.8 percentage points of total apparent SoC increase during the 10:00-15:00 field test on 8 June 2026. The 6 V medium panel and mini panel reached only 0.5 percentage points per hour in the same test window. These findings indicate that panel nominal voltage cannot be used alone to select a solar panel for IoT battery charging. Designers should consider active panel area, probable current capability under load, charger input limits, voltage regulation, and field validation. Future work should add current, irradiance, and temperature sensors to quantify actual energy output in watt-hours and to support statistical comparison over multiple days.

Overall, the study contributes a practical decision rule for early-stage solar IoT design: panel selection should be validated as an integrated charging subsystem rather than accepted from the nominal voltage label alone. The finding does not imply that all 9 V panels will outperform all 6 V panels, because panel construction, irradiance, orientation, regulator efficiency, battery state, and load profile can change the result. It does show, however, that a larger panel with suitable voltage regulation can provide a much stronger apparent recovery path for a single-cell IoT battery than smaller direct-connected panels under the tested conditions. For journal-level development, the next step is to transform this preliminary field screening into a repeatable energy-balance experiment by adding current sensing, irradiance measurement, panel temperature logging, matched initial battery conditions, and multi-day statistical comparison. These improvements would allow future research to quantify not only which node produces a higher voltage-derived apparent response, but also why, how efficiently, and under what operating limits the selected configuration can support sustainable IoT deployment.

ACKNOWLEDGMENT

The authors thank all parties who supported hardware assembly, ADC calibration, field testing, and data preparation for the solar-powered IoT monitoring nodes.

AI DISCLOSURE STATEMENT

AI-assisted language tools were used during manuscript revision to improve readability, structure, grammar, and academic clarity. The authors reviewed, verified, and approved the final content. All data interpretation, scientific claims, conclusions, and responsibility for the manuscript remain with the authors.

AUTHOR CONTRIBUTION

SHS conceptualization, methodology, field experiment design, supervision, data interpretation, and writing - original draft. IMR hardware assembly, firmware implementation, data acquisition, ADC calibration, and validation. MRAMS IoT system integration, Google Sheets data logging, visualization, and technical documentation. S experimental support, field testing, data curation, and formal analysis. RMS literature review, manuscript editing, reference checking, and writing - review and editing. All authors read and approved the final manuscript.

CONFLICT OF INTEREST STATEMENT

The authors declare that they have no known competing financial interests or personal relationships that could have appeared to influence the work reported in this paper.

REFERENCES

[1] G. C. G. Melo, I. C. Torres, I. B. Q. Araujo, D. B. Brito, and E. A. Barboza, "A low-cost IoT system for real-time monitoring of climatic variables and photovoltaic generation for smart grid application," Sensors, vol. 21, no. 9, p. 3293, 2021. https://doi.org/10.3390/s21093293

[2] Y. Cheddadi, H. Cheddadi, F. Cheddadi, F. Errahimi, and N. Es-sbai, "Design and implementation of an intelligent low-cost IoT solution for energy monitoring of photovoltaic stations," SN Applied Sciences, vol. 2, p. 1165, 2020. https://doi.org/10.1007/s42452-020-2997-4

[3] B. E. Demir, "A new low-cost Internet of Things-based monitoring system design for stand-alone solar photovoltaic plant and power estimation," Applied Sciences, vol. 13, no. 24, p. 13072, 2023. https://doi.org/10.3390/app132413072

[4] N. Rouibah, L. Barazane, M. Benghanem, and A. Mellit, "IoT-based low-cost prototype for online monitoring of maximum output power of domestic photovoltaic systems," ETRI Journal, vol. 43, no. 3, pp. 459-470, 2021. https://doi.org/10.4218/etrij.2019-0537

[5] B. H. Hameed and S. Kurnaz, "Secure low-cost photovoltaic monitoring system based on LoRaWAN network and artificial intelligence," Discover Computing, vol. 27, p. 36, 2024. https://doi.org/10.1007/s10791-024-09475-0

[6] W. He and M. T. Iqbal, "Power consumption minimization of a low-cost IoT data logger for photovoltaic system," Journal of Electronics and Electrical Engineering, vol. 2, no. 2, p. 241, 2023. https://doi.org/10.37256/jeee.2220233795

[7] Z. Tsiropoulos, I. Gravalos, E. Skoubris, V. Poulek, T. Petrik, and M. Libra, "A comparative analysis between battery- and solar-powered wireless sensors for soil water monitoring," Applied Sciences, vol. 12, no. 3, p. 1130, 2022. https://doi.org/10.3390/app12031130

[8] F. M. E. Haroun, S. N. M. Deros, A. A. Alkahtani, and N. M. Din, "Towards self-powered WSN: The design of ultra-low-power wireless sensor transmission unit based on indoor solar energy harvester," Electronics, vol. 11, no. 13, p. 2077, 2022. https://doi.org/10.3390/electronics11132077

[9] M. Grossi, "Energy harvesting strategies for wireless sensor networks and mobile devices: A review," Electronics, vol. 10, no. 6, p. 661, 2021. https://doi.org/10.3390/electronics10060661

[10] A. Sharma and A. Kakkar, "A review on solar forecasting and power management approaches for energy-harvesting wireless sensor networks," International Journal of Communication Systems, vol. 33, no. 8, e4366, 2020. https://doi.org/10.1002/dac.4366

[11] J. Singh, R. Kaur, and D. Singh, "Energy harvesting in wireless sensor networks: A taxonomic survey," International Journal of Energy Research, vol. 45, pp. 118-140, 2021. https://doi.org/10.1002/er.5816

[12] G. K. Ijemaru, K. L.-M. Ang, and J. K. P. Seng, "Wireless power transfer and energy harvesting in distributed sensor networks: Survey, opportunities, and challenges," International Journal of Distributed Sensor Networks, 2022. https://doi.org/10.1177/15501477211067740

[13] B. R. Paudyal and A. G. Imenes, "Investigation of temperature coefficients of PV modules through field measured data," Solar Energy, vol. 224, pp. 425-439, 2021. https://doi.org/10.1016/j.solener.2021.06.013

[14] J. M. Alvarez, D. Alfonso-Corcuera, E. Roibas-Millan, J. Cubas, J. Cubero-Estalrrich, A. Gonzalez-Estrada, R. Jado-Puente, M. Sanabria-Pinzon, and S. Pindado, "Analytical modeling of current-voltage photovoltaic performance: An easy approach to solar panel behavior," Applied Sciences, vol. 11, no. 9, p. 4250, 2021. https://doi.org/10.3390/app11094250

[15] O. A. Afolabi and E. R. Sadiku, "Design and implementation of a low-cost datalogger for solar irradiance and PV module temperature," Journal of Electrical Systems and Information Technology, vol. 11, p. 59, 2024. https://doi.org/10.1186/s43067-024-00180-y

[16] N. Li, Y. Zhang, F. He, L. Zhu, Y. Chen, J. Shen, and Y. Zhang, "Review of lithium-ion battery state of charge estimation," Global Energy Interconnection, vol. 4, no. 6, pp. 619-630, 2021. https://doi.org/10.1016/j.gloei.2022.01.003

[17] H. M. Hussein, A. Aghmadi, M. S. Abdelrahman, S. M. S. H. Rafin, and O. Mohammed, "A review of battery state of charge estimation and management systems: Models and future

prospective," WIREs Energy and Environment, vol. 13, no. 1, e507, 2024. https://doi.org/10.1002/wene.507

[18] Y. Yang, Q. Zhou, L. Zhang, D. Du, M. Zheng, Q. Niu, L. Gao, and X. Yuan, "Recent progresses in state estimation of lithium-ion battery energy storage systems: A review," Transactions of the Institute of Measurement and Control, vol. 47, no. 15, 2025. https://doi.org/10.1177/01423312221124354

[19] D. Hercog, T. Lerher, M. Truntic, and O. Tezak, "Design and implementation of ESP32-based IoT devices," Sensors, vol. 23, no. 15, p. 6739, 2023. https://doi.org/10.3390/s23156739

[20] A. I. Sukowati and L. M. Rahmah, "Density-optimized lookup table with piecewise linear interpolation for ESP32 ADC precision enhancement," Journal Zetroem, vol. 8, no. 1, pp. 56-64, 2026. https://doi.org/10.36526/ztr.v8i1.7602

[21] W. J. G. Gomes and D. Dinushka, "Low-cost ESP32-based smart 18650 Li-ion battery charger with IoT monitoring," Journal of Manufacturing Engineering, vol. 21, no. 1, pp. 006-010, 2026. https://doi.org/10.37255/jme.v21i1pp006-010

[22] I. A. Lazuardi, I. W. Farid, and C. W. Priananda, "Automatic transfer switch dilengkapi fitur monitoring website pada on-grid solar home system," Jurnal Teknik ITS, vol. 10, no. 2, 2021. https://doi.org/10.12962/j23373539.v10i2.68713

[23] A. Arifa, Suharno, M. Kamaruddin, and D. Harjunowibowo, "Enhancing measuring reliability: Calibration and validation of IoT-based DC power logger," Journal of Engineering and Applied Technology, vol. 6, no. 1, 2025. https://doi.org/10.21831/jeatech.v6i01.83282

[24] S. Tirones and Y. Hu, "Design and validation of portable low-cost ESP32-C6 based data acquisition for real-time power monitoring and experimental data collection," Diyala Journal of Engineering Sciences, vol. 19, no. 2, 2026. https://doi.org/10.24237/djes.2026.19201

[25] A. Yuan, S. S. Berutu, R. Saputra, and R. S. Sakoikoi, "Design and development of an IoT-based monitoring system for solar phone charging stations," Infact: International Journal of Computers, vol. 9, no. 2, 2025. https://doi.org/10.61179/infact.v9i02.775

[26] M. A. P. Kusumojakti and U. Zaky, "Deteksi real-time kondisi baterai menggunakan sistem monitoring berbasis perangkat bergerak," Jurnal Informatika Teknologi dan Sains, vol. 6, no. 4, 2024. https://doi.org/10.51401/jinteks.v6i4.4866

[27] Espressif Systems, "ESP32 series datasheet," Espressif Systems, 2026. [Online]. Available: https://documentation.espressif.com/esp32_datasheet_en.html. [Accessed: 01-Jul-2026].

[28] WEMOS Electronics, "D32 documentation," WEMOS Electronics, 2026. [Online]. Available: https://www.wemos.cc/en/latest/d32/d32.html. [Accessed: 01-Jul-2026].

[29] NanJing Top Power ASIC Corp., "TP4056: 1A standalone linear Li-ion battery charger datasheet," 2021. [Online]. Available: https://www.tp4056.com/datasheet/. [Accessed: 01-Jul-2026].

[30] Texas Instruments, "INA219 zero-drift, bidirectional current/power monitor with I2C interface datasheet (Rev. G)," Texas Instruments, 2014. [Online]. Available: https://www.ti.com/product/INA219. [Accessed: 01-Jul-2026].